PHYSICAL REVIEW B **77**, 041402(R) (2008)

Ab initio prediction of stable boron sheets and boron nanotubes: Structure, stability, and electronic properties

Xiaobao Yang, Yi Ding, and Jun Ni*

Department of Physics and Key Laboratory of Atomic and Molecular Nanoscience (Ministry of Education), Tsinghua University, Beijing 100084, People's Republic of China

(Received 19 June 2007; revised manuscript received 29 November 2007; published 2 January 2008)

Using first-principles calculations, we predict a novel stable boron sheet and boron nanotubes which show various electronic properties. The boron sheet is flat and has the structure that the two centers of each three hexagons in the hexagonal lattice are filled with additional atoms, which preserves the symmetry of the triangular lattice. The boron sheet is metal, and there are bands similar to the π bands in the graphene near the Fermi level. Rolled from the sheet, the nanotubes with diameter larger than 17 Å are metals. Smaller nanotubes are semiconductors with the gap decreasing as the diameter and chiral angle increase.

DOI: 10.1103/PhysRevB.77.041402 PACS number(s): 61.46.Fg, 31.15.A−, 68.65.−k

Carbon nanotubes have attracted wide attention due to their novel electronic properties and great potential of applications.[1,2] The tubes can be considered as a rolled graphene sheet, which can be either metals or semiconductors depending on their diameters and chiral vectors.[3–5] There are also other nanotubes synthesized, which can be of pure element (Au,[6] Bi,[7] Si,[8]…) or be formed from compounds (BC_3,[9] BN,[10] MoS_2,[11]…). However, except carbon nanotubes, most of the other nanotubes are quite simplex in electronic properties, being either all metal or all semiconductor.

Boron, the fifth element in the periodic table, possesses a richness of chemistry second only to carbon. Elemental boron has a variety of crystal structures containing multicenter bonds, which is a result of an electron deficiency. In contrast to the covalent, ionic, van der Waals, and metallic bonds, the multicenter bonds is a complex bonding type, which is important due to its existence in abundant compounds.[12,13] The α-rhombohedral bulk is the most stable boron structures, where boron atoms form a highly symmetric icosahedral cluster in a crystalline state.[14] Contrary to the bulk boron compounds, boron clusters B_n with $n<20$, prefer to be planar. B_{12} has the biggest largest highest occupied and lowest unoccupied molecular orbital (HOMO-LUMO) gap (~2.0 eV) and is therefore predicted to be very stable.[15] Like benzene, B_{12} has a symmetrical bond distribution and is highly aromatic. When $n \geqslant 20$, for example, the most stable structure for B_{20} is a double-ring tubular structure, which can be considered as the embryo of the single-walled boron nanotubes.[16] Recently, the most stable structure of B_{80} has been predicted, which is a hollow cage and more stable than the double rings.[17] Theoretical and experimental research have been performed on boron sheet and boron nanotubes. Ciuparu *et al.* reported the synthesis of single-walled boron nanotubes with diameters in the range of 3 nm.[18] The structural details of boron single-walled nanotubes have attracted great attention. It is reported that the buckled triangular boron sheet is more stable compared to boron planar structures and the energy per atom is 0.48–0.58 eV higher than the α-rhombohedral bulk.[19–21] The boron nanotubes rolled from the buckled triangular sheet are large deformed.[19]

One of the main difficulties in synthesizing boron nanotubes appears to be the instability of a graphenelike boron sheet. Recent reports focus on the boron sheet constructed as the triangular lattice. However, the large deformation and buckling show that the triangular boron sheet is not very stable. Thus, the most stable structure of boron sheets is unclear. The stable structure of the planar sheet will help in constructing the hollow cage and nanotubes.

In this paper, we show a novel stable boron flat sheet. The energy per atom measured with respect to the α-rhombohedral bulk is only 0.38 eV, which is the most stable boron sheet studied so far. The boron tubes rolled from the sheet are more stable than the B_{80} cage. Significantly, the predicted boron nanotubes, similar to carbon nanotubes, can be either metal or semiconductor dependent on diameter and chirality.

We have performed the calculations of the total energies of the boron sheet and boron nanotubes using the VASP (Vienna *ab initio* simulation package).[22] The approach is based on an iterative solution of the Kohn-Sham equations of the density-functional theory in a plane-wave basis set with Vanderbilt ultrasoft pseudopotentials.[23] We use the exchange correlation with the generalized gradient approximation given by Perdew and Wang.[24] We set the plane-wave cutoff energy to be 320 eV and the convergence of the force on each atom to be less than 0.01 eV/Å. Both the interlayer separation for boron sheet and the intertubular distance for boron nanotubes are set to be 9 Å, which is enough to make the systems isolated. The Monkhorst-Pack scheme is used to sample the Brillouin zone.[25] The optimization of the lattice constants and the atom coordinates is made by minimization of the total energy. The boron sheet is fully relaxed with a mesh of $9\times9\times1$ and the mesh of **k** space is increased to $20\times20\times1$ to obtain the accurate energies with atoms fixed after relaxations. A mesh of $1\times1\times9$ is used for the relaxation of the boron nanotubes with small lattice constants, and $1\times1\times20$ is used for the static calculations. For the system with large lattice constants, meshes of $1\times1\times3$ and $1\times1\times10$ are used for relaxation and static calculation, respectively.

Graphene sheets, carbon nanotubes, and carbon clusters have similarly constructed units because of sp^2 hybridization. However, there has been no graphenelike boron sheet

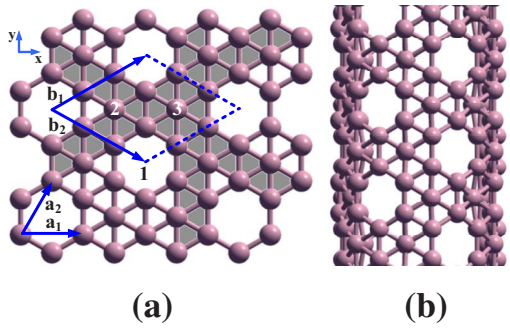

FIG. 1. (Color online) (a) The structure of boron sheet and (b) the structure of boron nanotubes. The (3,3) tube is shown as an example.

observed, which might be one of the main difficulties in synthesizing boron nanotubes. We analyze the possible configurations to construct the stable boron sheet. The first one is the graphenelike sheet. The lattice vector for the graphenelike sheet is $\mathbf{a}_1,\mathbf{a}_2$ as is shown in Fig. 1(a). This sheet is unstable since there are only six electrons for each boron atom. Previous works[19–21] considered the boron sheet to be a triangular lattice, which is the hexagonal sheet with every center of hexagons filled with additional atoms. According to recent reports, the most stable B_{80} cluster is symmetrically similar to the C_{60} structure with an additional atom at the center of each hexagon.[17] The B_{92} completely built with triangular bonding units are less stable than the B_{80} cluster cage. Thus we consider the boron sheet of the hexagonal lattice with the two centers of each three hexagons filled with additional atoms as is shown in Fig. 1(a). The lattice vector for this sheet is $\mathbf{b}_1,\mathbf{b}_2$. The unit cell of this sheet contains three unit cells of the hexagonal lattice. Here 2,3 are the filled sites of the hexagonal lattice and vacancies (site 1) form a $(\sqrt{3}\times\sqrt{3})R$ 30° pattern. Many experimental and theoretical researches on small boron clusters, such as icosahedral B_{12} and the cluster family of boron double rings with various diameters,[15–17] show that the boron double rings are stable to construct clusters. This boron sheet can be considered as interlaced double rings, as is shadowed in Fig. 1(a). The sheet preserves the symmetry of the triangular lattice, and the energy per atom measured with respect to the α-rhombohedral bulk is only 0.38 eV, showing it is more stable than the other sheet predicted before.[19–21] The length l_{B-B} of B-B bonds is 1.67 Å, which equals approximatively the shorter ones (1.677 Å) in the stable B_{80} cage.[17] In this stable boron sheet, 3/4 of boron atoms have five nearest neighbors and 1/4 of boron atoms have six nearest neighbors, which is the same ratio as the stable B_{80} cage. The boron sheet remains flat when the relaxation of supercells is made and the buckled initial configurations are used. The hexagonal pyramid units are planar, similar to the B_{80} cage.

Boron is an electron deficient element and the multicenter bonds are found in boron structures. We obtained the charge difference of the boron sheet by subtracting the charge density of boron atom from that of the sheet, as is shown in Fig. 2(a). The multicenter bonds are formed among four boron atoms, as is marked by $A1$, $A2$, $B1$, and $B2$. From the figure, we can see that 3/4 of boron atoms have the nearest B-B

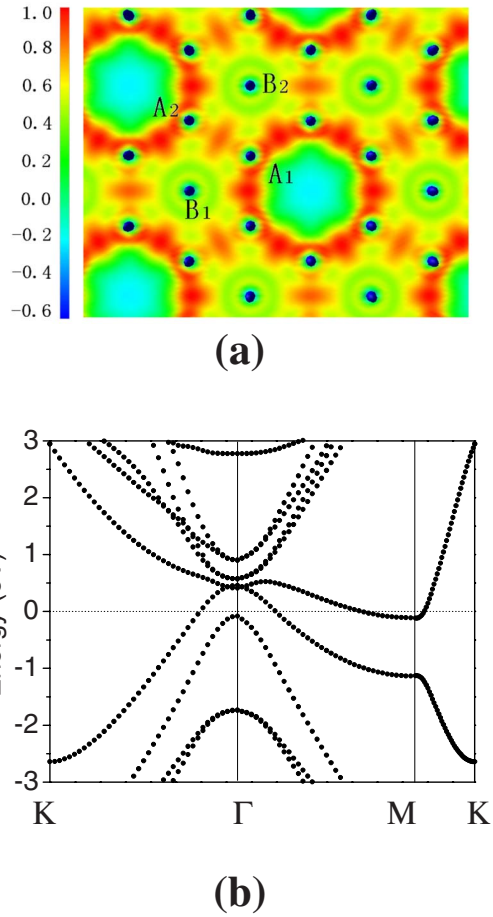

FIG. 2. (Color online) (a) The charge difference of the boron sheet and (b) the band structure of the boron sheet.

bonds ($A1$-$A2$) and 1/4 of boron atoms form the bonds with the next-nearest boron atoms ($B1$-$B2$). This is one of the reasons why this boron sheet is more stable than the other sheets. Figure 2(b) shows the band structure of the boron sheet. There are bands similar to the π bands in the graphene near the Fermi level, which is degenerated at the Γ point about 0.5 eV above the Fermi level.

Boron nanotubes can be rolled from the stable boron sheet and the (3,3) boron tubes are shown in Fig. 1(b) as an example. There are two kinds of vectors to determine the boron nanotubes: the primary vectors of the hexagonal lattice used for carbon nanotubes and the primary vectors of boron sheet lattice. For the hexagonal lattice, $\mathbf{a}_1=a\mathbf{x}$, $\mathbf{a}_2=a\left(\frac{1}{2}\mathbf{x}+\frac{\sqrt{3}}{2}\mathbf{y}\right)$, $a=\sqrt{3}l_{B\text{-}B}$. For the boron sheet lattice, $\mathbf{b}_1=b\left(\frac{1}{2}\mathbf{x}+\frac{\sqrt{3}}{2}\mathbf{y}\right)$, $\mathbf{b}_2=b\left(\frac{1}{2}\mathbf{x}-\frac{\sqrt{3}}{2}\mathbf{y}\right)$, $b=3l_{B\text{-}B}$. To satisfy $p\mathbf{b}_1+q\mathbf{b}_2=n\mathbf{a}_1+m\mathbf{a}_2$, the chiral vector (p,q) of the boron sheet lattice corresponds to the vector (n,m) of the hexagonal lattice with $p=(n+2m)/3$ and $q=(n-m)/3$. Thus, the $(p,0)$ boron nanotube corresponds to the (n,n) $(n=p)$ carbon nanotube and the (p,p) boron nanotube corresponds to the $(n,0)$ $(n=3p)$ carbon nanotube. The lattice constants are enlarged since the unit cell of the $(p,0)$ boron nanotubes contains three unit cells of the (n,n) $(n=p)$ carbon nanotubes.

We have performed calculations on the boron nanotubes

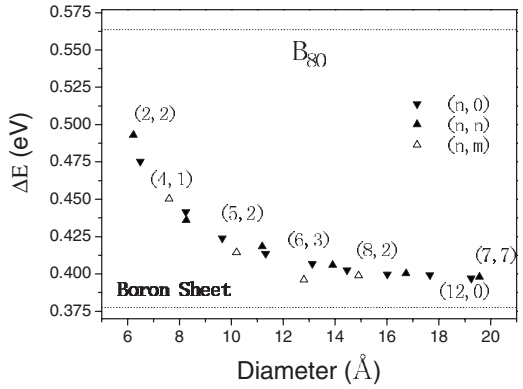

FIG. 3. The relative formation energies of the boron nanotubes vs the diameters. The formation energy per atom is measured with respect to the α-rhombohedral bulk (6.27 eV). The energies of B_{80}, the buckled triangular boron sheet, and the boron sheet we predicted are plotted for comparisons.

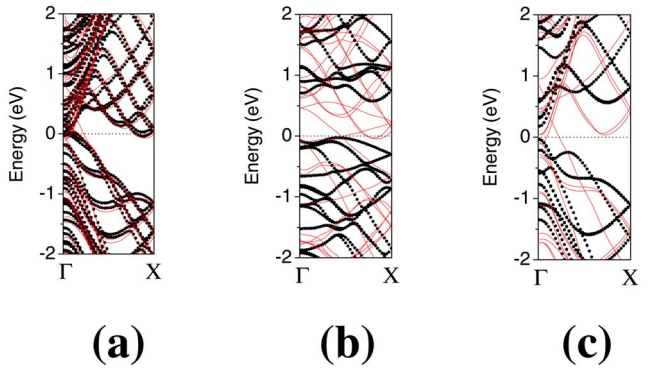

FIG. 5. (Color online) Band structures of boron nanotubes (a) for the (7,7) tube, (b) for the (5,0) tube, and (c) for the (3,3) tube. The bands plotted with black dots are obtained from first-principles calculations and red lines from zone folding. The Fermi level is set to zero.

with different diameters 6–20 Å and various chiral vectors. When the boron sheet is rolled into boron nanotubes, some of the hexagonal pyramid units are not planar for boron nanotubes with small diameters. For the large tubes, the hexagonal pyramid units tend to be planar. We have calculated the relative formation energies (ΔE) as measured with respect to the α-rhombohedral bulk (6.27 eV). As is shown in Fig. 3, the relative formation energy decreases from 0.49 eV to 0.39 eV as the diameter increases. The (2,2) tube with highest relative formation energy is still more stable than B_{80}.[17] We have calculated the boron nanotubes rolled from the puckered triangular lattice for comparison, which are large deformed during the relaxations.[19,20] However, there is no obvious deformation during the relaxations of our predicted boron nanotubes and the tubes tend to be columnar as the diameter increases, similar to the carbon nanotubes.

We have calculated the electronic structures of the $(p,0)$ $(p=4-11)$ tubes, (p,p) $(p=2-7)$ tubes, and (p,q) tubes. The gap as a function of diameter is shown in Fig. 4. Previous theoretical works showed that the boron nanotubes rolled from the triangular lattice are always metallic.[19] However, our predicted boron nanotubes show various electronic properties, which can be either metals or semiconductors with different gaps. For the diameters larger than 17 Å, most the tubes are metals. The diameter of boron nanotubes synthesized is 36±1 Å.[18] When the diameters of the tubes are smaller than 17 Å, the $(p,0)$ boron tubes are semiconductors and the band gap of the $(p,0)$ $(p=4-9)$ tubes decreases from 0.77 eV to 0.27 eV as the diameter increases. The (p,p) $(p=3-5)$ tubes are semiconductors with direct gaps from 0.21 eV to 0.11 eV. For the tubes with similar diameters, the gap decreases as the chiral angle increases because the $(p,0)$ tubes have largest gaps while the (p,p) tubes have smallest gaps.

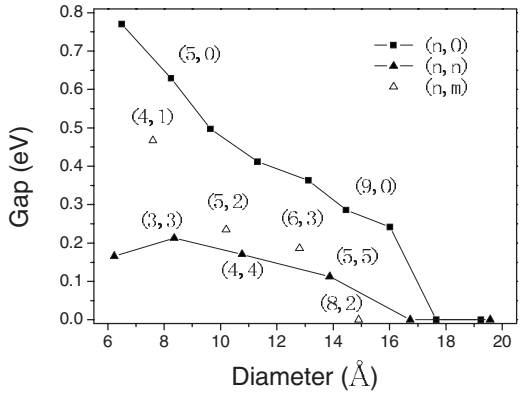

FIG. 4. The gap of the boron nanotubes as a function of diameter.

As is shown in Fig. 2(b), there are bands similar to the π bands in the graphene near the Fermi level, which is degenerated at the Γ point about 0.5 eV above the Fermi level. There are several intersections between the Fermi level and bands. Thus, the zone-folding features for boron nanotubes would be more complex as compared to the carbon nanotubes.[26] For larger tubes, band structures obtained by zone folding are in agreement with the ones obtained from first-principles calculations. For example, the (7,7) tube is metal as shown in Fig. 5(a). For smaller tubes, band structures obtained by zone folding show that the tubes are metals while the first-principles calculations show that the tubes are semiconductors. For example, the (5,0) tube is a semiconductor with indirect gap as shown in Fig. 5(b). The energy bands of the (3,3) tube are shown in Fig. 5(c) as an example of semiconducting tubes with direct gap. Zone folding cannot explain the semiconducting of boron nanotubes, which is due to the change of structure. For example, the (3,3) boron tubes can be constructed by adding 12 atoms on every cell of the (9,0) carbon nanotube structure. We found that the distances from the adding atoms to the axis are divided into two groups: 3.75 Å and 4.20 Å. When rolled from a sheet containing two inequivalent triangular lattices, the tubes are semiconducting due to the symmetry breaking.[8] For boron tubes with similar diameters, the distance difference of inequivalent atoms decreases as the chiral angle increases, which explains the gap variation with the chirality. For large

tubes, the distance difference of inequivalent atoms tends to be zero and the tubes are metal.

In summary, we have investigated the electronic and structural properties of a novel boron sheet and the relative boron nanotubes. The sheet is flat and preserves the symmetry of the triangular lattice. The sheet and the boron nanotubes rolled from the sheet are more stable than the stable B_{80} cage. They are the most stable sheets and nanotubes so far. The boron sheet is a metal and the nanotubes can be either metals or semiconductors (gap 0.1–0.8 eV) dependent on diameter and chirality. Similar to the carbon nanotubes, our predicted boron sheet and nanotubes have various electronic properties, which may have potential applications in the fabrication of novel nanoelectronic devices.

Note added. Another work addressing the same boron sheet was published recently.[27]

This research was supported by the National Natural Science Foundation of China (Grants Nos. 10474049 and 10674076) and the National Basic Research Program of China (Grant No. 2006CB605105).

*junni@mail.tsinghua.edu.cn

[1] S. Iijima, Nature (London) **354**, 56 (1991).
[2] R. H. Baughman, A. A. Zakhidov, and W. A. de Heer, Science **297**, 787 (2002).
[3] N. Hamada, S. I. Sawada, and A. Oshiyama, Phys. Rev. Lett. **68**, 1579 (1992).
[4] J. W. G. Wildoer, L. C. Venema, A. G. Rinzler, R. E. Smalley, and C. Dekker, Nature (London) **391**, 59 (1998).
[5] T. W. Odom, J. L. Huang, P. Kim, and C. M. Lieber, Nature (London) **391**, 62 (1998).
[6] R. T. Senger, S. Dag, and S. Ciraci, Phys. Rev. Lett. **93**, 196807 (2004); Y. Oshima, A. Onga, and K. Takayanagi, *ibid.* **91**, 205503 (2003).
[7] Y. Li, J. Wang, Z. Deng, Y. Wu, X. Sun, D. Yu, and P. Yang, J. Am. Chem. Soc. **123**, 9904 (2005).
[8] X. Yang and J. Ni, Phys. Rev. B **72**, 195426 (2005); M. De Crescenzi, P. Castrucci, and M. Scarselli, Appl. Phys. Lett. **86**, 231901 (2005).
[9] D. L. Carroll, Ph. Redlich, X. Blase, J.-C. Charlier, S. Curran, P. M. Ajayan, S. Roth, and M. Rühle, Phys. Rev. Lett. **81**, 2332 (1998); Y. Miyamoto, A. Rubio, S. G. Louie, and M. L. Cohen, Phys. Rev. B **50**, 18360 (1994).
[10] H. J. Xiang, J. Yang, J. G. Hou, and Q. Zhu, Phys. Rev. B **68**, 035427 (2003); E. Bengu and L. D. Marks, Phys. Rev. Lett. **86**, 2385 (2001).
[11] G. Seifert, H. Terrones, M. Terrones, G. Jungnickel, and T. Frauenheim, Phys. Rev. Lett. **85**, 146 (2000); R. Tenne, L. Margulis, M. Genut, and G. Hodes, Nature (London) **360**, 444 (1992).
[12] A. Janotti and C. G. Van de Walle, Nat. Phys. **6**, 44 (2007).
[13] X. Li *et al.*, Science **315**, 356 (2007).
[14] M. Fujimori, T. Nakata, T. Nakayama, E. Nishibori, K. Kimura, M. Takata, and M. Sahata, Phys. Rev. Lett. **82**, 4452 (1999).
[15] H.-J. Zhai *et al.*, Nat. Phys. **2**, 827 (2003).
[16] B. Kiran *et al.*, Proc. Natl. Acad. Sci. U.S.A. **102**, 961 (2005).
[17] N. Gonzalez Szwacki, A. Sadrzadeh, and B. I. Yakobson, Phys. Rev. Lett. **98**, 166804 (2007).
[18] D. Ciuparu, R. F. Klie, Y. Zhu, and L. Pfefferle, J. Phys. Chem. B **108**, 3967 (2004).
[19] J. Kunstmann and A. Quandt, Phys. Rev. B **74**, 035413 (2006); Chem. Phys. Lett. **402**, 21 (2005); I. Boustani and A. Quandt, J. Chem. Phys. **110**, 3176 (1999);
[20] M. H. Evans, J. D. Joannopoulos, and S. T. Pantelides, Phys. Rev. B **72**, 045434 (2005).
[21] K. C. Lau and R. Pandey, J. Phys. Chem. C **111**, 2906 (2007); K. C. Lau, R. Pati, R. Pandey, and A. C. Pineda, Chem. Phys. Lett. **418**, 549 (2006).
[22] G. Kresse and J. Hafner, Phys. Rev. B **47**, 558 (1993); Phys. Rev. B **49**, 14251 (1994); G. Kresse and J. Furthmüller, Comput. Mater. Sci. **6**, 15 (1996); Phys. Rev. B **54**, 11169 (1996).
[23] D. Vanderbilt, Phys. Rev. B **41**, 7892 (1990).
[24] J. P. Perdew, J. A. Chevary, S. H. Vosko, K. A. Jackson, M. R. Pederson, D. J. Singh, and C. Fiolhais, Phys. Rev. B **46**, 6671 (1992).
[25] H. J. Monkhorst and J. D. Pack, Phys. Rev. B **13**, 5188 (1976).
[26] R. Saito, G. Dresselhaus, and M. Dresselhaus, *Physical Properties of Carbon Nanotubes* (Imperial College Press, London, 1998).
[27] H. Tang and S. Ismail-Beigi, Phys. Rev. Lett. **99**, 115501 (2007).